Alinejad et al. Tissue Engineering part A. vol 25, 2019 (accepted draft)

Injectable Chitosan Hydrogels with Enhanced Mechanical Properties for Nucleus Pulposus Regeneration

Yasaman Alinejad [*1,2,3], Atma Adoungotchodo [*1,2,3], Michael P Grant [3], Laura M Epure [3], John Antoniou[3,4], Fackson Mwale [3,4], Sophie Lerouge [&,1,2]

[1]Laboratory of Endovascular Biomaterials (LBeV), Centre de recherche du CHUM (CRCHUM), 900 St Denis St, Montreal, QC, H2X 3H8, CANADA
[2]Department of Mechanical Engineering, École de technologie supérieure (ETS), 1100 Notre-Dame West, Montreal, QC, H3C 1K3, CANADA
[3]Lady Davis Institute for Medical Research, SMBD-Jewish General Hospital, 5790 Ch de la Côte-des-Neiges, Suite H-421, Montreal, QC, H3S 1Y9, CANADA
[4]Division of Orthopaedic Surgery, McGill University, 1650 Ave. Cedar, Montreal, QC, H3G 1A4, CANADA

*: Authors contributed equally

[&:] **Corresponding author**
Sophie Lerouge, Ph.D.
Laboratory for endovascular biomaterials (LBeV)
CHUM research center (CRCHUM), 900 St Denis St,
Montreal, QC H2X 3H8, Canada
Tel: + 1 (514) 396-8836; fax: +1 514 412 7785
E-mail: sophie.lerouge@etsmtl.ca

Version accepted by Tissue Engineering, Part A, in 2018

Running title: **Chitosan-based scaffolds for IVD repair**

Keywords: Intervertebral disc, Nucleus pulposus, Chitosan, Hydrogel, Mechanical properties

ABSTRACT

Intervertebral disc (IVD) degeneration has been implicated as a major component of spine pathology. As the IVD degenerates, the tissue becomes dehydrated, fibrotic, fissured, acellular, and calcified. These changes can lead to disc bulging, herniation, Schmorl's Nodes, inflammation and hyperinnervation. Injectable hydrogels have received much attention in recent years as scaffold for seeding cells to replenish disc cellularity and restore disc properties and function. However, they generally present poor mechanical properties. In this study, we investigate several novel thermosensitive chitosan (tsCH) hydrogels for their ability to mimic the mechanical properties of the nucleus pulposus (NP) tissue while being injectable, able to entrap and maintain viability of NP cells, and retain matrix proteins. These new hydrogels were prepared by mixing chitosan (CH) with various combinations of three gelling agents: sodium hydrogen carbonate (SHC) and/or beta-glycerophosphate (BGP) and/or phosphate buffer (PB). The kinetics of gelation were studied at room and body temperature by rheology. Mechanical properties of the hydrogels were characterized under compression and torsion and compared with human NP tissue. NP cells were seeded in the hydrogel when still liquid at room temperature (RT), prior to its gelation at 37°C. Hydrogel cytocompatibility and functionality was assessed by measuring cell viability, metabolism, and proteoglycan synthesis. Although all the proposed hydrogels exhibited enhanced strength compared to CH-BGP thermosensitive hydrogels and suitable cytocompatibility and rheological properties, one formulation (containing 2% chitosan, 7.5mM of SHC and 0.1M of BGP) showed mechanical properties similar to human NP tissue, and stimulated better the synthesis and retention of proteoglycans from NP cells. Thus, this novel tsCH hydrogel shows promise for IVD regeneration.

Impact statement:
A thermosensitive chitosan-based hydrogel was developed which mimics the mechanical properties of the human nucleus pulposus (NP) tissue and provides a suitable environment for seeded NP cells to live and produce glycosaminoglycans. This scaffold is injectable through 25G needle and rapidly gels in vivo at body temperature. It has the potential to restore mechanical properties and stimulate biological repair of degenerated intervertebral disc (IVD), and could therefore be used for the minimally-invasive treatment of IVD, which degeneration affects more than 1 person out of 5 in the world.

INTRODUCTION

Intervertebral discs (IVDs) are highly organized avascular structures with a complex poro-elastic and anisotropic behavior[1]. They consist of a peripheral collagen-rich annulus fibrosus (AF) surrounding the inner proteoglycan-rich central nucleus pulposus (NP)[2]. Two thin cartilaginous endplates confine the IVD and link it to the vertebral bodies [3]. Although AF and NP have very distinct biomechanical and biochemical properties [4], they function as a load-bearing unit, allowing for complex spinal motion [5] and large cyclic loading [6]. The NP is thought to resist compressive forces through its high content in aggrecan [4] which induce a high swelling pressure that provides much of the compressive stiffness. The AF collagen network helps immobilize proteoglycans within the tissue and provides tensile and shear properties [4].

IVDs degeneration is one of the main causes of low back pain, the most common type of pain restricting daily activity of elderly and working population [7]. As the IVD degenerates, NP loses water and changes from a gelatinous to a more fibrotic structure with the appearance of fissures in both NP and AF. Current first line treatment approaches are targeted to pain management (e.g. drugs, analgesics, physiotherapy). Patients with late stage disease and pain refractory to medication are treated surgically (i.e. disc excision and vertebral fusion) which offers short-term pain relief in many instances but alters spinal mechanics leading to subsequent adjacent-level disc degeneration and elevated early failure rates [8, 9]. Therefore, regenerative strategies for biological repair of the degenerated IVD have received much attention in the recent years. One attractive approach is to supplement the disc with cells and/or bioactive factors within an injectable scaffold with suitable characteristics for the IVD tissue [10]. This scaffold can not only enhance the retention of the cells and the ECM components they produce, but can also offer mechanical support during the regeneration process.

The ideal scaffold for the biological repair of the NP should (a) be injectable through small needles to avoid surgeries and large incision that may damage the AF (b) present rapid solidification after injection to avoid leakage, (c) possess mechanical properties consistent with the native tissue, (d) be biocompatible (e) biodegradable (f) porous to ensure cellular penetration and adequate diffusion of nutrients to cells and to the extra-cellular matrix formed by these cells. and (g) retain the glycosaminoglycans (GAGs) synthesized by the cells.

Several biomaterials have been tested as injectable scaffolds for IVD repair, including polyglycolic acid [11], collagen and collagen/hyaluronan scaffolds [12, 13], agarose [14], alginate [15], and chitosan (CH) [16]. However, some of them do not retain GAGs [12, 17] and they usually lack the suitable mechanical properties. Among them CH-based scaffolds however appear as promising candidates.

CH is an amino-polysaccharide obtained by the alkaline deacetylation of chitin, widely used for tissue engineering applications. Its structural similarities to GAGs and hydrophilic nature make it an attractive IVD scaffold [16, 18, 19]. CH in association with a weak base, such as beta-glycerophosphate (BGP), can form thermosensitive injectable hydrogels [20]. These CH-BGP hydrogels have however limited cytocompatibility, low mechanical properties, and the BGP is substrate for alkaline phosphatase which is known to induce mineralization [21]. It was recently proven that these limitations can be overcome by either removal of BGP or its addition at lower concentrations in formulations with additional gelling agents [22], namely

sodium hydrogen carbonate (SHC) and phosphate buffer (PB). These new CH-based hydrogels are thermosensitive, injectable, cytocompatible and much stronger than conventional CH-BGP hydrogels. Moreover, their gelation rate, osmolality and mechanical strength can be adjusted according to their formulation [23].

The objective of the present study was to identify a suitable CH thermosensitive hydrogel scaffold for biologic repair of the NP. Several formulations of CH physical hydrogels were selected, based on their mechanical properties, gelation kinetics and cytocompatibility [23] and were evaluated to identify the formulation that exhibits NP-like mechanical properties, good injectability through small diameter needle, excellent viability of encapsulated NP cells and the ability to stimulate and retain the produced GAGs.

MATERIALS AND METHODS

Chitosan hydrogel preparation

CH (Shrimp shell chitosan, Kitomer, PSN 326-501, Premium Quality, Mw 250 kDa, DDA 94%, Marinard Biotech, Rivière-au-Renard, QC, Canada) was first purified, freeze-dried, ground and sieved as previously described [22]. The purified CH powder was then solubilized in HCl (0.1 M) at 3.33% (w/v) and the obtained solution was sterilized by autoclaving (20 min, 121 °C) and stored at 4°C.
β-Glycerol phosphate disodium salt pentahydrate ($C_3H_7Na_2O_6P \cdot 5H_2O$, hereafter BGP), sodium phosphate monobasic NaH_2PO_4 (SPM) and sodium phosphate dibasic Na_2HPO_4 (SPD) were purchased from Sigma-Aldrich (Oakville, ON, Canada). Sodium hydrogen carbonate $NaHCO_3$ (sodium bicarbonate, hereafter SHC) was purchased from MP Biomedicals (Solon, OH, USA).

BGP, SHC and phosphate buffer (PB, pH = 8, prepared with NaH_2PO_4 and Na_2HPO_4 at a ratio of 0.06 w/w in milli-Q water) were combined at different concentrations (Table 1). For cell experiments, the solutions were sterilized by filtration through 0.22 µm filters.

Hydrogels were prepared by mixing the CH acidic solution with the gelling agent (GA) solution at 3:2 (v/v) ratio using syringes connected to each other through a female-to-female luer-lock syringe connector. For cell experiments and osmolality measurements, CH solution was first mixed with doubled concentrated GA solution at 3:1 (v/v) ratio, then the CH-GA mixture was mixed with the content of a third syringe containing complete culture medium with or without cells at 4:1 (v/v) ratio.

Selection of the chitosan hydrogel formulations

Three gel compositions (Table 1) were selected based on our previous work showing their appropriate characteristics such as mechanical properties, gelation kinetics and cytocompatibility [22, 23]. In addition, BGP0.4 hydrogel was chosen as control because of its ideal gelation kinetic and injectability through small lumen [14, 16]. CH was maintained at similar concentration in all selected hydrogel formulations (i.e. 2% w/v). Hydrogels are therefore coded according to their final molar concentrations of gelling agent in their formulations (e.g. SHC0.075BGP0.1 corresponds to a gel containing 2% (w/v) CH, 0.075M SHC and 0.1M BGP).

Hydrogels characterization

Rheological properties

Rheological properties at both room temperature (RT, 22°C) and body temperature (37 °C) were investigated using an Anton Paar instrument (Physica MCR 301, Germany) with coaxial cylinder geometry (CC10/T200) in the linear viscoelastic region (strain and frequency at 5% and 1Hz respectively). The complex viscosity (η*), storage (G') and loss (G'') moduli were followed immediately after mixing the gel components (hydrogel mixture: 1.5 mL). Gelation time was defined as the time of crossover of G' and G''[24].

Mechanical properties

Sample preparation: Directly after mixing, the hydrogel solutions were poured into cylindrical containers (12mm height, 14mm diameter) and incubated for 24h at 37°C prior to mechanical testing.

Human lumbar spines were obtained through the organ donation program of Hema-Québec. NP tissue (6.9 ± 0.4 mm height and 12 ± 3.1 mm diameter) from three lumbar discs (Thompson grade 3) were isolated from a donor (age 44) and used for the mechanical testing. All procedures were approved by our institutional review board.

Unconfined compression: Mechanical properties of the hydrogels were measured on the hydrogel samples (12mm height, 14mm diameter) by unconfined compression test with Bose Electroforce® 3200 equipped by a 225N load cell. Unconfined compression was performed at 100%/min until 50% deformation to determine stress versus strain curve and the secant modulus.

Relaxation tests: To compare mechanical properties of the hydrogels with those of human NP tissue, the equilibrium modulus in unconfined compression was determined using incremental stress relaxation test, as previously defined by Cloyd et al. [25]. Compression was applied by increments of 5% strain at 5%/s followed by 5 min relaxation, until reaching 25% strain. The equilibrium stress at each relaxation step was plotted to trace the stress-strain curves, the slope of which defines as the equilibrium modulus. The samples (5mm height, 14mm diameter) were immersed in phosphate buffered saline (PBS) during the test to avoid dehydration.

Dynamic shear stress: Torsional shear test was performed with Anton Paar rheometer on hydrogel samples prepared in 6-well plates (1 mL), using a plate-plate geometry with a rough upper plate to avoid sliding. An initial 10% compression was applied to make contact between the sample and the upper plate. The complex modulus of hydrogel was measured in the linear viscoelastic region at a constant strain of 1% and different frequencies (1, 10 and 100 rad/s). Sample height was (1.4 ± 0.1 mm) for SHC0.075PB0.02, (1.8 ± 0.4 mm) for SHC0.075BGP0.1 and (2 ± 0.2 mm) for SHC0.075PB0.04.

Osmolality measurements

The osmolality (Advanced® Micro Osmometer 3300, Advanced Instruments Inc.) was measured on hydrogel filtrates, obtained by pressing the hydrogels with 0.45 μm filters after 24h gelation at 37°C.

Hydrogels cytocompatibility

Cell isolation and culturing

NP cells were recovered from the NP region of the bovine coccygeal IVDs of healthy 22-28-month-old steers by sequential digestion with 0.125% Pronase and 0.2mg/mL Collagenase [26]. After isolation, the cells were expanded and used for study within passage 4 using Dulbecco's Modified Eagle's Medium (DMEM, low glucose: 1g/L) supplemented with 10% fetal bovine serum (FBS) and 1% penicillin/streptomycin (P/S).

For all cell experiments, gels containing cells were prepared by mixing the hydrogel solution and cell suspension, deposited in 48 well plates (0.5 mL per well) through a syringe (without a needle) and the culture medium was added after 3 minutes of gelation (Hydrogel/media 1:1 ratio). Hydrogels without cells were used as blanks. Culture media was changes every 3 days.

NP cells viability and metabolic activity in the hydrogels

Cell viability in the hydrogels (10^6 cells per mL) was investigated by LIVE/DEAD assay. After 14 days of culture, hydrogels were washed once with PBS, incubated with the LIVE/DEAD Cell Imaging Kit (Life technologies) reagent for 30 min, and then observed by confocal microscopy (Zeiss LSM confocal laser-scanning microscope equipped with 488 nm and 543 nm laser lines). Ten z-stacked images were merged representing 100 μm thickness. The ratio of live cells (green) to total number of cells (green and red) was calculated using the cell counter function in ImageJ (National Institute of Health, USA) in four merged images per condition.

The metabolic activity of the encapsulated cells was evaluated using Alamar Blue (AB) assay (Biotium, 10%v/v) after 3, 7 and 14 days of culture. Moreover, the hydrogels containing cells were incubated with chitosanase solution (Sigma-Aldrich, 0.3U/mL in PBS+0.1%BSA, pH=5) for 24h at 37°C and the DNA content was measured in the solution using the PicoGreen assay (Quant-iT™ PicoGreen™ dsDNA Assay Kit, Thermo Fisher, Waltham, MA) according to the manufacturer instructions.

GAG synthesis and retention

The total amount of GAG synthesized (released in the media and retained in the gel) by the encapsulated cells in the hydrogels ($4x10^6$ cells per mL of hydrogel) was quantified using a modified 1,9-dimethylmethylene blue (DMMB) dye-binding assay (Sigma-Aldrich) following 7 days of culture. The culture media was changed every third day, and the GAG released into the media was analyzed as cumulative GAG release. GAG retention in the hydrogels was evaluated at 7 days. Acellular hydrogels were used as controls. Absorbance was read at 570 nm, immediately following the addition of DMMB. Chondroitin sulfate A sodium salt from bovine trachea (Sigma-Aldrich) was used to create the standard curve. Samples were diluted to fall within the middle of the linear range of the standard curve.

Injectability in human NP

Two human lumbar IVDs were isolated from lumbar spines of two donors (51 and 52 years old). One of the best hydrogel formulations in terms of rheological and mechanical properties as well as GAG retention (i.e. SHC0.075PB0.02, see results section) was colored during preparation with a drop of toluidine blue (Sigma-Aldrich) to facilitate visualization. The hydrogel solution (0.5 mL for donor 1 and 0.3 mL for donor 2) was injected though 25-gauge needle into the center of the IVDs through AF. After 30 min incubation at 37℃, discs were transected, macroscopically graded [27] and examined for hydrogel repartition and/or possible extrusion within the IVD.

Statistical analysis

Results are reported as mean ± standard error mean (SEM). Statistical analysis was performed using the GraphPad Prism (version 7.0; GraphPad Software, Inc., La Jolla, CA, USA) program. Differences between the gels were assessed with one-way or two-way repeated analysis of variance (ANOVA) followed by a post hoc Tukey's multiple comparison test.

RESULTS

Rheological properties

Rheological properties were studied at RT to evaluate the injectability of the hydrogel solution and at body temperature to determine their gelation kinetics once injected. All tested hydrogel formulations showed relatively low complex viscosity immediately after mixing at 22°C (Figure 1A). SHC0.075BGP0.1 and SHC0.075PB0.02 were the most stable (viscosity still less than 5 Pa.s after 30 min at RT) suggesting easy injectability of the hydrogel solution through small needles and catheters during all this period. In contrast, the viscosity of SHC0.075PB0.04, and more especially BGP0.4, increased more rapidly, suggesting a possible maximum delay for injection after mixing. This difference between the gels was confirmed by the evolution of their storage moduli (G') at 22°C (Figure 1B).
The G' values of all hydrogels at 37°C increased at a much higher rate than at RT (Figure 2), confirming their thermosensitive character. While all tested hydrogels exhibited rapid gelation time (G'=G'' at $t < 15s$), their gelation kinetics slightly differed depending on their formulation (The intersection of G' and G'' is not shown in the figure as the first datapoint is taken at 15s). The initial storage moduli of BGP0.4 and SHC0.075PB0.02 was relatively low (less than 100 Pa), but rapidly increased as a function of time, reaching 1200 kPa and 2850 kPa after 1 h respectively. Both SHC0.075BGP0.1 and SHC0.075PB0.04 presented higher initial G', and reached more than 4000 kPa after 1h at 37°C.

Mechanical properties of hydrogels using unconfined compression and dynamic shear

Unconfined compression test performed on fully-formed hydrogels showed that the new hydrogel formulations presented strongly enhanced resistance to compression compared to BGP0.4 (Figure 3A). Moreover, they withstood compressive forces up to 50% deformation without breakage, while BGP0.4 samples broke between 20% and 30% deformation.
Since the hydrogels presented a viscoelastic behavior, the secant modulus in compression was determined as the slope of a line connecting the point of zero strain to a point at a specified deformation (Figure 3B). At 15% deformation (the maximum physiological deformation of the IVD [28]), the secant moduli of SHC0.075BGP0.1, SHC0.075PB0.02 and SHC0.075PB0.04 hydrogels were respectively 5, 4 and 4 fold higher than that of BGP0.4 hydrogel. At 50% deformation, the secant moduli of SHC0.075BGP0.1 and SHC0.075PB0.02 (>120 kPa) were significantly higher ($p \leq 0.01$ and $p \leq 0.05$ respectively) compared to SHC0.075PB0.04 (≈95kPa).

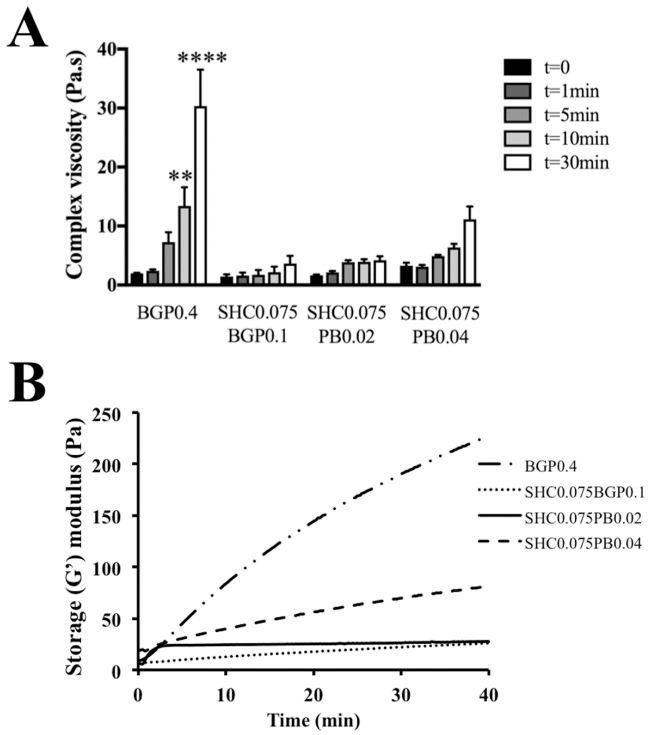

Figure 1. Novel hydrogel formulations are more stable at RT than BGP0.4 hydrogel. *(A) Evolution of complex viscosity with time at 22°C immediately after mixing. Mean ± SEM (n=3). **p<0.01, ****p<0.0001 compared to t=0 for each formulation. (B) Evolution of storage modulus (G') with time at 22°C. Mean (n=3).*

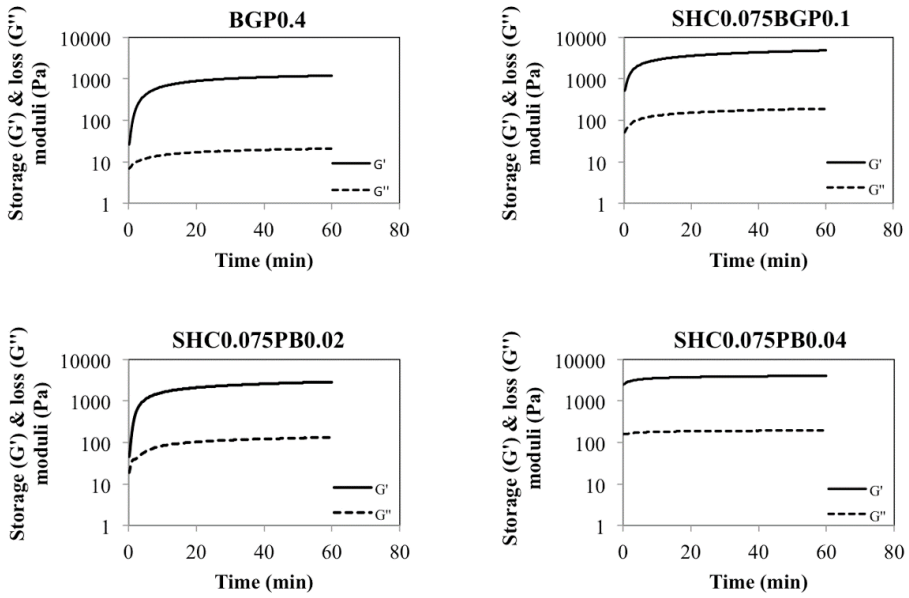

Figure 2. Chitosan hydrogels are thermosensitive with rapid kinetic of gelation. *Evolution of storage (G') and loss (G'') moduli with time at 37 °C (strain 5%, frequency 1 Hz) immediately following preparation. Mean (n=3-4)*

The incremental stress-relaxation unconfined compression test confirmed that SHC0.075BGP0.1 exhibited the highest mechanical properties, followed by SHC0.075PB0.02 (Figure 4). Both gels exhibited an equilibrium modulus similar to the human NP tissue (6.1±1.7 kPa, in agreement with the values previously reported in the literature (5.2±2.56 kPa[25]), while SHC0.075PB0.04 and BGP0.04 had significantly lower values ($p<0.001$).

Finally, the complex shear moduli (G*) of SHC0.075BGP0.1, SHC0.075PB0.02 and SHC0.075PB0.04 hydrogels were found to range from 7 to 14 kPa (Figure S1, supplementary data). These values were similar to human NP (7-21 kPa [29]) and over 14 to 25 fold higher than BGP0.4 ($P<0.001$). No statistically significant differences were observed between the complex shear moduli measured at different angular velocities for each hydrogel.

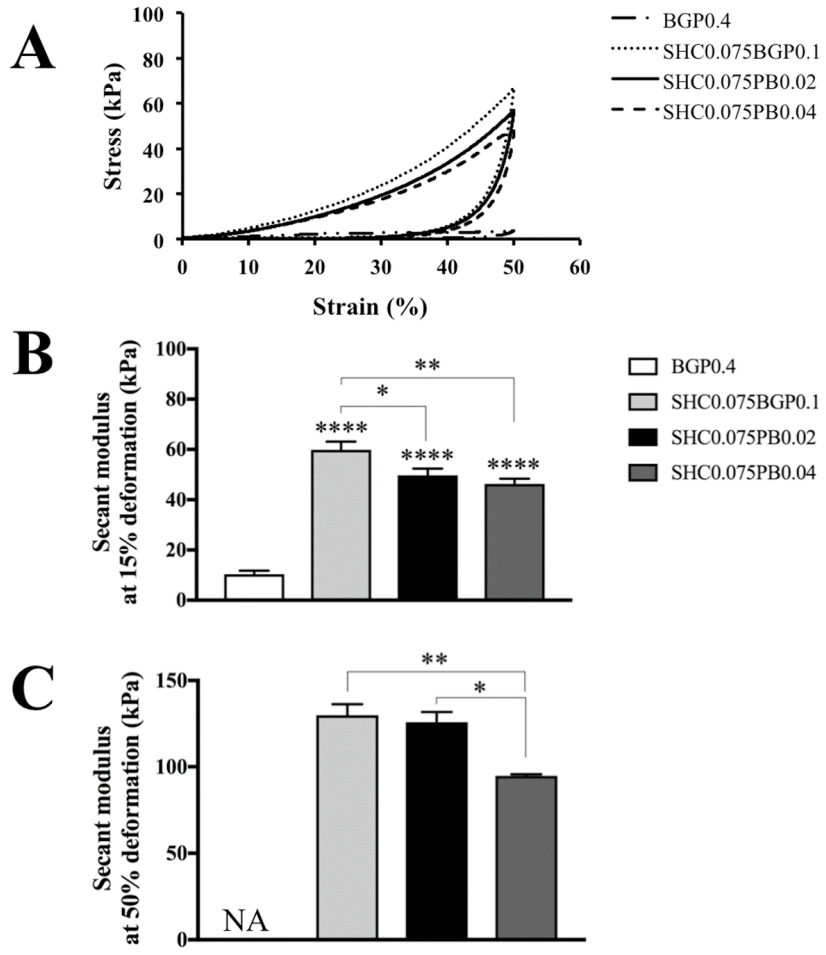

Figure 3. Novel hydrogel formulations are more resistant to compressive forces than BGP0.4 hydrogel. *(A) Mean stress-strain curve of the hydrogels in unconfined compression test (after 24h at 37 °C) (n=3-5). (B) Secant modulus of the hydrogels in unconfined compression test at 15% deformation and (C) at 50% deformation (BGP0.4 hydrogels did not withstand 50% deformation and they are shown as not applicable (NA) in the graph). Mean ± SEM (n=3-5). *p<0.05, **p<0.01, ****p<0.0001 compared to BGP0.4 and between hydrogels (using bars).*

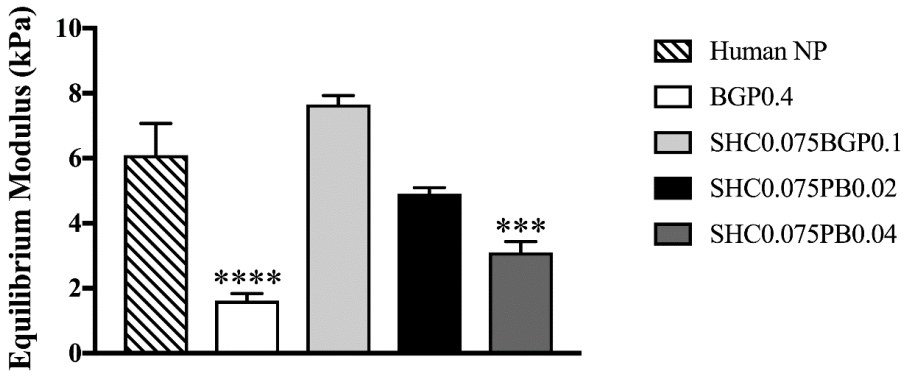

Figure 4. SHC0.075BGP0.1 and SHC0.075PB0.02 hydrogels show mechanical properties like human NP tissue*. Equilibrium moduli of hydrogels measured using incremental stress relaxation during unconfined compression (Five steps of 5% strain at 5%/s, followed by 5min of relaxation in PBS). Mean ± SEM (n = 5-6). ***P < 0.001, ****P < 0.0001 compared to human NP tissue.*

Osmolality

The BGP0.4 hydrogel was hypertonic (>800 mOsmol/L), while the osmolality of SHC0.075BGP0.1 was close to IVD osmolality (≈430 mOsmol/L) and other formulations were slightly hypotonic for IVD (<430mOsm/L) (Table 1) [30]. Part of these values (estimated to 158 mOsmol/L) is due to the culture media added with the cells in the hydrogels [23].

Cytocompatibility of the hydrogels with disc cells

The cytocompatibility of the hydrogels was studied by monitoring the viability, metabolic activity and DNA content of NP cells encapsulated and maintained in culture for 14 days in the different hydrogel formulations. Figure 5A shows representative LIVE/DEAD images after 14 days and Figure 5B shows the percentage of viable cells. Very low viability (16%) was observed for cells encapsulated in BGP0.4 hydrogel after 14 days. Contrarily, NP cells demonstrated significantly higher levels of cell viability in the new hydrogel formulations. Cell survival was greater than 80% in SHC0.075BGP0.1 and SHC0.075PB0.02 hydrogels. Cells encapsulated in the new formulations also showed significantly higher metabolic activity (Figure 5C) and DNA content after 14 days of incubation (Figure 5D) compared to cells encapsulated in BGP0.4 hydrogel.

In addition, alamar blue assay performed after 3, 7 and 14 days showed that except BGP0.4 formulation which had a cytotoxic effect, no loss of metabolic activity was observed between day 3, 7 and 14 in the cells encapsulated in new formulations indicating that they did not have any cytotoxic effect on NP cells (Figure 2, supplementary data).

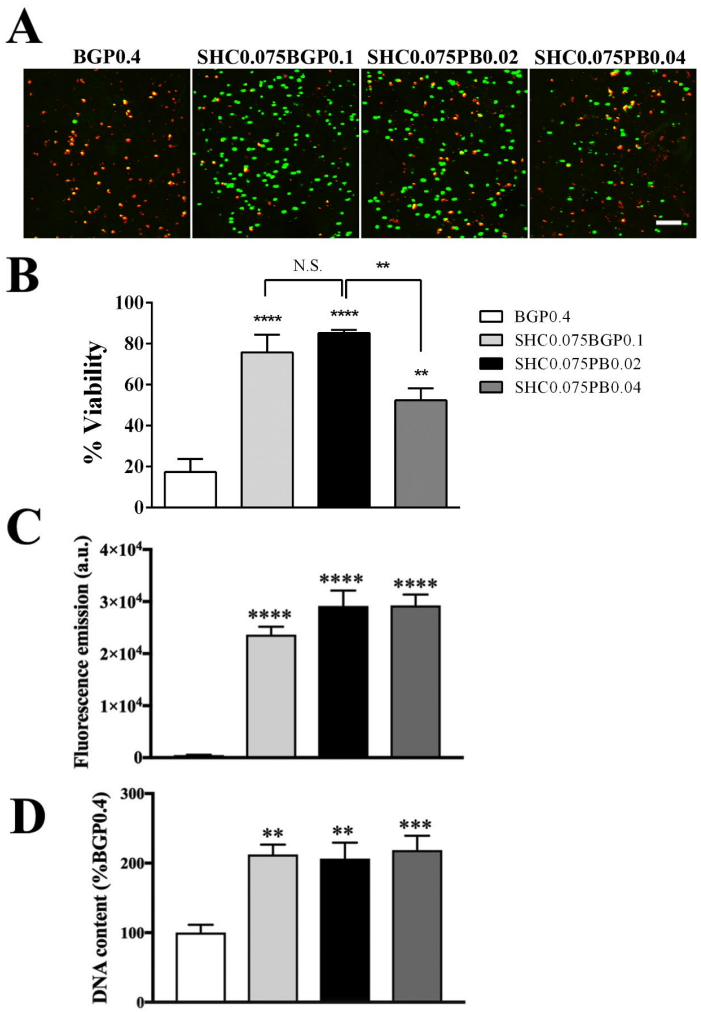

Figure 5. Cytocompatibility of the chitosan hydrogels. *(A) LIVE/DEAD assay performed on cells encapsulated in hydrogels and cultured for 14 days. Scale bar represents 100 µm. (B) Percentage of viable cells according to cell counting on LIVE/DEAD images. Mean ± SEM (n = 4). (C) Metabolic activity of the cells encapsulated in hydrogels after 14 days. Mean ± SEM (n = 9). (D) DNA content in the cell-laden hydrogels after 14 days (expressed as percentage of DNA content in the BGP0.4 hydrogel). Mean ± SEM (n = 9). ** p<0.01, *** p<0.001, **** p<0.0001 compared to BGP0.4 and between hydrogels (using bars).*

GAG synthesis by the encapsulated NP cells

Proteoglycans are an integral component of the intervertebral disc. They are important in providing its unique mechanical properties and maintaining hydrostatic pressure. This is largely due to their glycosaminoglycan chains[31]. To determine whether our novel hydrogel preparations could generate a suitable scaffold for proteoglycan synthesis by NP cells, the constructs were cultured for 7 days and the content of extractable proteoglycans both released in the media and retained in the hydrogels was quantified by the DMMB assay (Figure 6). Cells encapsulated in SHC0.075BGP0.1 and SHC0.075PB0.02 produced significantly higher amounts of GAG compared to cells encapsulated in SHC0.075PB0.04 and BGP0.4 hydrogels (Figure 6A). The total amount of GAG was higher in SHC0.075BGP0.1 hydrogel compared to SHC0.075PB0.02 (Figure 6B). Interestingly, both the SHC0.075BGP0.1 and SHC0.075PB0.02 hydrogels retained similar amounts of GAG (Figure 6B).

Hydrogels injectability in human NP

To confirm the feasibility of injecting the hydrogel into the NP through a 'clinical size' needle and observe how the hydrogel solution distributes into the clefts of degenerated human disks (Thomson grade 3), one of the best formulations, SHC0.075PB0.02 hydrogel was injected into two human cadaveric IVDs through a 25G syringe and incubated for 30 min at 37°C (Figure 7). Macroscopic observation of the disc shows that the hydrogel flowed into the nuclear clefts with no detectable leakage through the AF and out of the disc.

A

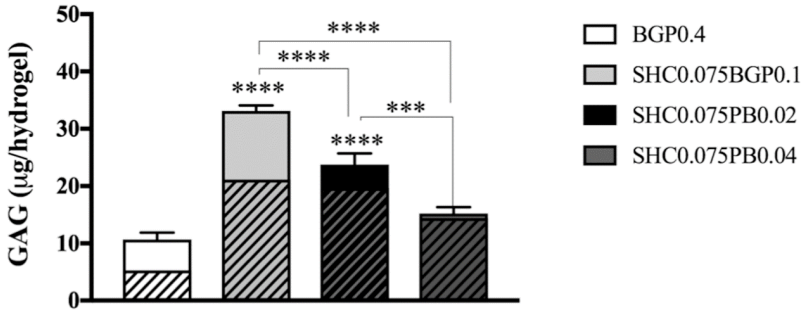

B

Hydrogel	Total (µg)	Released (µg)	Accumulated in hydrogel (µg)
BGP0.4	10.7±1.2	5.7±0.5	5.2±0.7
SHC0.075BGP0.1	33.1±0.9	12.1±1.2	21.0±1.1
SHC0.075PB0.02	23.8±1.9	4.1±0.4	19.6±1.6
SHC0.075PB0.04	15.2±1.1	0.8±0.2	14.3±1.2

Figure 6. GAG production and retention in hydrogels. *(A) Total GAG synthesized by encapsulated NP cells for 7 days (GAG accumulated in the hydrogels is presented as patterned area). Mean ± SEM (n = 9). (B) Table of Total GAG synthesized, accumulated in hydrogels and released in medium (measured in µg). Mean ± SEM (n = 9). For total GAG, *** p<0.001, **** p<0.0001 compared to BGP0.4 and between hydrogels (using bars). For accumulated GAG, + p<0.05, ++ p<0.01 and ++++ p<0.0001 compared to BGP0.4 and between hydrogels (using bars).*

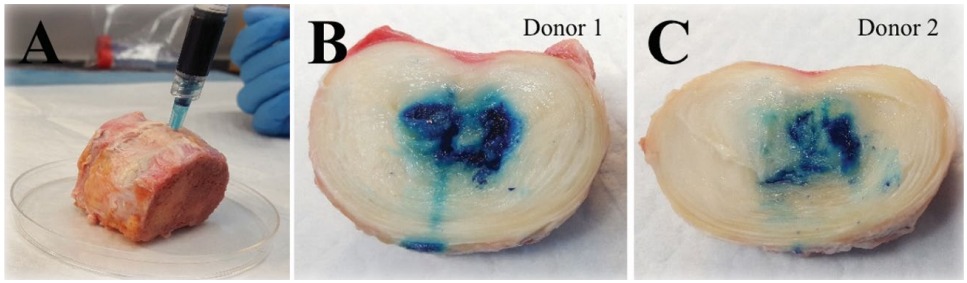

Figure 7. SCH0.075PB0.02 hydrogel was injected into human degenerated IVD. *(A) Injection of the toluidine blue-stained hydrogel into the degenerated NP of human cadaveric degenerated IVD (grade 3) using a 25-gauge needle. (B&C) Macroscopic evaluation of an axially dissected disc following 30 minutes incubation at 37℃ for donor 1 and 2. Note that the solution filled the nuclear clefts and no evidence of hydrogel (blue) extrusion was observed.*

DISCUSSION

Recent works have established the proof of concept of cell therapy for IVD repair in order to reestablish IVD homeostasis and reverse the degeneration process [32, 33]. Several clinical trials have been already performed or are in progress [34-39], a few with injectable biomaterials as cell carrier, [34, 38, 39]. Those carriers (atelocollagen, fibrin, hyaluronic acid and hyaluronic acid derivative gels) [32], however, present very poor mechanical properties. As recently reviewed by Bowles and Setton (2017), promising results have been obtained with other biomaterials in vitro and in animal models [40-42]. Among them, several CH containing matrices have been reported [16, 43-45]. However, most of them present limited mechanical properties [46-49] and the search for a suitable injectable scaffold which could not only increase cell retention but could also help initial restauration of disk height and mechanical properties is still ongoing. A few materials were capable of presenting both injectability and suitable mechanical strength. They are mostly multiple component networks, containing CH as well as other proteins, polymers and/or bioactive agents [50-52]. In comparison, the injectable hydrogels presented in this study are simple, without protein, bioactive agent or chemical product, which may be an advantage in terms of FDA approval.

The three novel hydrogels tested in this work (SHC0.075BGP0.1, SHC0.075PB0.02, SHC0.075PB0.04) allowed injection in liquid form at RT, followed by rapid gelation at body temperature, reaching mechanical properties which were far above those of conventional CH-BGP thermogels (BGP0.4). Two of the new formulations (i.e. SHC0.075BGP0.1 and SHC0.075PB0.02) showed mechanical properties comparable to human NP tissue, both in compression and shear, suggesting their potential to restore the mechanical properties of the IVD, at least temporarily, before the injected cells create the new ECM.

Mimicking the mechanical properties of the native tissue is important[29], since a scaffold with lower mechanical properties cannot withstand IVD load, while a scaffold with higher mechanical properties may induce instability and increase the degeneration rate [53].
These strong mechanical properties are one of the main advantages of these new scaffolds, as most of the physical injectable hydrogels, such as the previously studied CH-BGP hydrogels, are not mechanically strong enough for IVD regeneration requirements [16, 22]. Notably, the good mechanical properties of our hydrogels were obtained without any crosslinker. Previous work showed that this is due to the use of sodium hydrogen carbonate (SHC) at a precise concentration as gelling agent. CH-BGP physical hydrogel formation involves heat-induced protons transfer from CH to BGP. This results in CH chains neutralization, decreasing repulsive forces, and increasing attractive forces between CH chains [54]. In the case of SHC, the small size of the molecule and its decomposition in CO_2, may keep the chitosan chains closer during gelation, allowing formation of a stronger network. Its combination with either phosphate buffer or BGP enables to reach both good mechanical properties and rapid gelation kinetics [22], making them advantageous compared to previously developed CH physical thermogels made with BGP alone, sodium hydrogen carbonate [55] dibasic sodium phosphate [56] or ammonium hydrogen phosphate [57]. The absence of chemical initiators, crosslinkers, radiation and high temperature during gelation is favorable for cell survival and may facilitate clinical transfer, compared to many other hydrogel systems [58-61].

In the present study, we applied unconfined compression test to compare the mechanical properties of the hydrogels among each other, but also with that of isolated human NP tissue.

However, it should be noted that although unconfined compression test is widely applied in the literature to characterize the mechanical properties of the NP [25, 62, 63], it can only partially represent the mechanical strength of the NP tissue. Ideally, both confined and unconfined compressions are required to fully characterize a potential replacement of the NP because despite the fact that the NP is restricted by the AF and endplate cartilage in vivo, compressive load on the NP can be transferred to the AF when it expands radially. Therefore, physiologically the NP is neither completely confined nor completely unconfined [25]. In the future we plan to conduct ex-vivo test with injected hydrogel which will be more effective and relevant to conclude about the capability of the hydrogel to restore the mechanical properties of the degenerated IVD.

Another advantage of our two best gels (i.e. SHC0.075BGP0.1 and SHC0.075PB0.02) is their relative stability in liquid form at RT, which facilitates mixing of cells and therapeutic agents and provides a suitable time frame for manipulation and injection of the hydrogel. The novel CH thermogels also showed better cytocompatibility to the NP cells compared to conventional CH-BGP hydrogels, as shown by Live dead, AlamarBlue, DNA and GAG content. This improvement, previously observed with encapsulated fibroblastes [23], T lymphocytes [64] and mesenchymal stem cells[23], is likely due to the lower salt content of the new hydrogels. In the case of CH-BGP hydrogels, high concentrations of BGP are required to achieve rapid gelation kinetics, which results in cytotoxic effect on cells due to hyperosmolarity (≥800mOsm/L for BGP0.4 gels) [22, 65]. In the new formulations, the osmolality is close to physiological values (262 to 434 mOsm/L).
While knowing how the native cells would respond to the hydrogel is certainly a good first step, eventually the cytocompatibility of a more translationally relevant cell source (e.g. MSCs) will need to be evaluated prior to clinical translation.

The higher GAG production by NP cells observed in SHC0.075BGP0.1 (434mosm/L) compared to SHC0.075PB0.02 (262mosm/L) could be explained by its osmolality close to IVD's osmolality. Indeed, the intervertebral disc is hyperosmolar compared to other tissues (430-496 mOsm) [30, 66]. The expression level of aggrecan was shown to increase in hyperosmotic conditions (500 mOsm) in human NP and AF cells [67] as well as bovine NP cells [68]. Spillekom et al. found that expression of brachyury, a phenotypic indicator of the NP, as well as aggrecan and GAG synthesis was at optimal levels when cells were cultured in medium adjusted to 400 mOsm/L[69]. For this reason, even though SHC0.75PB0.02 also showed suitable kinetics of gelation, mechanical properties comparable to the human NP and, good cytocompatibility with the NP cells, SHC0.075GP0.1 showed in addition the ability to produce the highest GAG amount and therefore is the best of all tested hydrogel formulations for IVD repair.

The GAG production by encapsulated cells in three-dimensional hydrogels remains however considerably lower than in a mature NP [62]. In a normal bovine NP, the proteoglycan content increases with age from 3.1 to 4.7 mg/100 mg tissue [70]. It was shown that $2x10^6$ NP cells embedded in a collagen/hyaluronic scaffold cultured in DMEM supplemented by FCS and stimulated with TGFβ1/bFGF produce about 2% of the total GAG amount in mature NP after 20 days [70]. Therefore, it would be very interesting to evaluate the effect of stimulating factors/agents that can augment proteoglycan synthesis by NP and stem cells on the GAG production of the encapsulated cells.

CONCLUSION

In summary, new CH hydrogels, synthesized by mixing CH solution with sodium hydrogen carbonate in combination with phosphate buffer and BGP, were evaluated for their potential for biological repair of the NP. These physical hydrogels, made of polysaccharide biopolymers without chemical products, are thermosensitive, injectable and biodegradable. One of the tested formulations (SHC0.075BGP0.1) exhibited mechanical properties similar to the human NP tissue, provided the most suitable environment to maintain NP cells alive and active and was able to induce the highest GAG amount produced by the encapsulated cells and retained in the hydrogel. This formulation is a particularly promising candidate towards the development of biological repair strategies for the treatment of degenerated IVD.

Acknowledgements
Authors would like to thank funding organizations CIHR and NSERC (Collaborative Health Research Program 508365), as well as Canada research chair program (SL). YA and AA also acknowledge scholarships by the Fonds de recherche du Quebec (FRQS and FRQNT, respectively) and NSERC.

Disclosure Statement
The authors have no competing financial interests to disclose.

References

1. Vergroesen, P.-P.A., et al. Journal of biomechanics, 2016. **49**(6): p. 857-863.
2. Rannou, F., et al. EMC - Rhumatologie-Orthopédie, 2004. **1**(6): p. 487-507.
3. Freemont, A. Rheumatology, 2008. **48**(1): p. 5-10.
4. Antoniou, J., et al. Journal of Magnetic Resonance Imaging, 2013. **38**(6): p. 1402-1414.
5. Roughley, P.J. Spine, 2004. **29**(23): p. 2691-9.
6. Costi, J.J., et al. Expert review of medical devices, 2011. **8**(3): p. 357-376.
7. Chan, S. and B. Gantenbein-Ritter. Swiss Med Wkly, 2012. **142**: p. w13598.
8. Abramovitz, J.N. and S.R. Neff. Neurosurgery, 1991. **29**(2): p. 301-7; discussion 307-8.
9. Snider, R.K., et al. Clinical Spine Surgery, 1999. **12**(2): p. 107-114.
10. Blanquer, S., et al. Advanced drug delivery reviews, 2015. **84**: p. 172-187.
11. Mizuno, H., et al. Spine (Phila Pa 1976), 2004. **29**(12): p. 1290-7; discussion 1297-8.
12. Rong, Y., et al. Tissue Eng, 2002. **8**(6): p. 1037-47.
13. Alini, M., et al. Spine (Phila Pa 1976), 2003. **28**(5): p. 446-54; discussion 453.
14. Gruber, H.E., et al. Spine J, 2004. **4**(1): p. 44-55.
15. Chou, A.I. and S.B. Nicoll. J Biomed Mater Res A, 2009. **91**(1): p. 187-94.
16. Roughley, P., et al. Biomaterials, 2006. **27**(3): p. 388-396.
17. Grad, S., et al. J Biomed Mater Res A, 2003. **66**(3): p. 571-9.
18. Mwale, F., et al. Tissue engineering, 2005. **11**(1-2): p. 130-140.
19. Di Martino, A., et al. Biomaterials, 2005. **26**(30): p. 5983-5990.
20. Chenite, A., et al. Biomaterials, 2000. **21**(21): p. 2155-61.
21. Ishikawa, Y. and R.E. Wuthier. Bone and mineral, 1992. **17**(2): p. 152-157.
22. Assaad, E., et al. Carbohydrate Polymers, 2015. **130**: p. 87-96.
23. Ceccaldi, C., et al. Macromolecular Bioscience, 2017. **17**(6): p. 1600435.
24. Winter, H.H. and F. Chambon. Journal of rheology, 1986. **30**(2): p. 367-382.
25. Cloyd, J.M., et al. European Spine Journal, 2007. **16**(11): p. 1892-1898.
26. Gawri, R., et al. European cells & materials, 2012. **26**: p. 107-19.
27. Thompson, J.P., et al. Spine, 1990. **15**(5): p. 411-5.
28. Joshi, A., et al. Biomaterials, 2006. **27**(2): p. 176-184.

29. Iatridis, J.C., et al. Spine, 1996. **21**(10): p. 1174-1184.
30. van Dijk, B., et al. Tissue Engineering Part C: Methods, 2011. **17**(11): p. 1089-1096.
31. Urban, J. and A. Maroudas. Clinics in Rheumatic Diseases, 1980. **6**(1): p. 51-76.
32. Sakai, D. and J. Schol. Journal of Orthopaedic Translation, 2017. **9**: p. 8-18.
33. Huang, Y.C., et al. Spine J, 2013. **13**(3): p. 352-62.
34. Yoshikawa, T., et al. Spine, 2010. **35**(11): p. E475-E480.
35. Orozco, L., et al. Transplantation, 2011. **92**(7): p. 822-828.
36. Coric, D., et al. Journal of Neurosurgery: Spine, 2013. **18**(1): p. 85-95.
37. Noriega, D.C., et al. Transplantation, 2017. **101**(8): p. 1945-1951.
38. Kumar, H., et al. Stem Cell Research & Therapy, 2017. **8**(1): p. 262.
39. Tschugg, A., et al. Neurosurgical review, 2017. **40**(1): p. 155-162.
40. Bowles, R.D. and L.A. Setton. Biomaterials, 2017. **129**: p. 54-67.
41. Schutgens, E.M., et al. Eur Cell Mater, 2015. **30**: p. 210-31.
42. Hudson, K.D., et al. Current Opinion in Biotechnology, 2013. **24**(5): p. 872-879.
43. Richardson, S.M., et al. Biomaterials, 2008. **29**(1): p. 85-93.
44. Cheng, Y.H., et al. Tissue Eng Part A, 2010. **16**(2): p. 695-703.
45. Ghorbani, M., et al. Materials Science and Engineering C, 2017. **80**: p. 502-508.
46. Peroglio, M., et al. The Spine Journal, 2013. **13**(11): p. 1627-1639.
47. Vernengo, J., et al. Journal of Biomedical Materials Research Part B: Applied Biomaterials, 2008. **84B**(1): p. 64-69.
48. Richardson, S.M., et al. Biomaterials, 2008. **29**(1): p. 85-93.
49. Crevensten, G., et al. Annals of Biomedical Engineering, 2004. **32**(3): p. 430-434.
50. Gullbrand, S.E., et al. Acta Biomater, 2017. **60**: p. 201-209.
51. Zhu, Y., et al. Biomater Sci, 2017. **5**(4): p. 784-791.
52. Smith, L.J., et al. Tissue Engineering - Part A, 2014. **20**(13-14): p. 1841-1849.
53. Whatley, B.R. and X. Wen. Materials Science and Engineering: C, 2012. **32**(2): p. 61-77.
54. Lavertu, M., et al. Biomacromolecules, 2008. **9**(2): p. 640-650.
55. Liu, L., et al. International journal of pharmaceutics, 2011. **414**(1-2): p. 6-15.
56. Li, X., et al. Journal of Pharmaceutical Sciences, 2011. **100**(1): p. 232-241.
57. Nair, L.S., et al. Biomacromolecules, 2007. **8**(12): p. 3779-3785.
58. Kumar, D., et al. Acta biomaterialia, 2014. **10**(8): p. 3463-3474.
59. Xavier, J.R., et al. ACS nano, 2015. **9**(3): p. 3109-3118.
60. Priyadarshani, P., et al. Osteoarthritis and cartilage, 2016. **24**(2): p. 206-212.
61. Thorpe, A.A., et al. Acta Biomaterialia, 2016. **36**: p. 99-111.
62. Smith, L.J., et al. Tissue Engineering. Part A, 2014. **20**(13-14): p. 1841-1849.
63. Johannessen, W., et al. Transactions of the Orthopaedic Research Society, 2004. **29**: p. 1150.
64. Monette, A., et al. Biomaterials, 2016. **75**: p. 237-249.
65. Ahmadi, R. and J.D. de Bruijn. Journal of Biomedical Materials Research Part A, 2008. **86A**(3): p. 824-832.
66. Ishihara, H., et al. American Journal of Physiology-Cell Physiology, 1997. **272**(5): p. C1499-C1506.
67. Wuertz, K., et al. Journal of Orthopaedic Research, 2007. **25**(11): p. 1513-1522.
68. Neidlinger-Wilke, C., et al. Journal of Orthopaedic Research, 2012. **30**(1): p. 112-121.
69. Spillekom, S., et al. Tissue Engineering Part C: Methods, 2014. **20**(8): p. 652-662.
70. Alini, M., et al. Spine 2003. **28**(5): p. 446-54.

SUPPLEMENTARY DATA

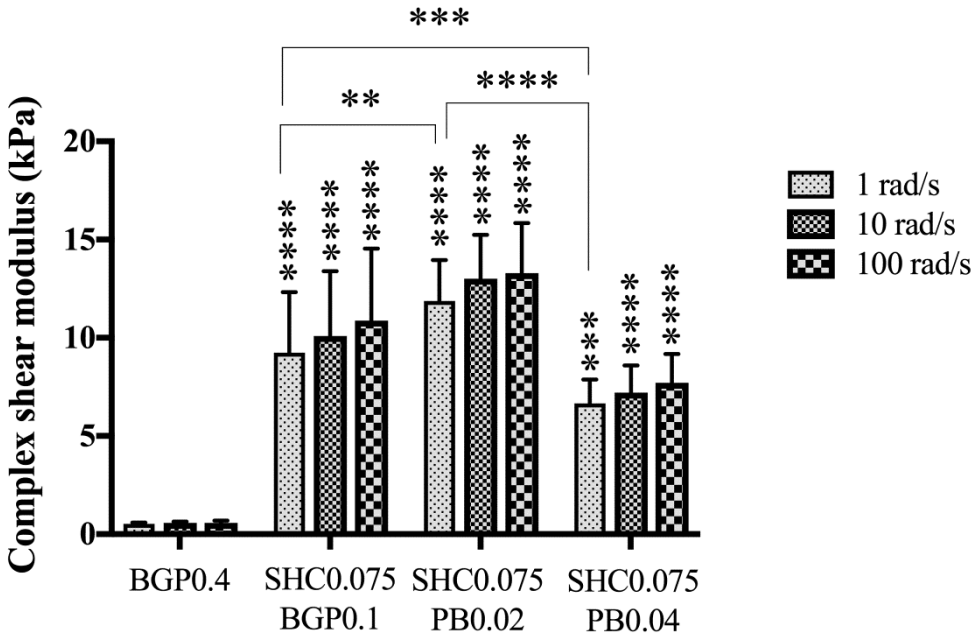

Figure S1. **Torsional shear: complex shear modulus measured at fixed shear stress amplitude of 1% and various frequencies**. Data are shown as mean ± SD (N=5, n=1). * shows statistically significant difference compared to BGP0.4 at the same angular velocity. *P<0.05, **P<0.01, ***P<0.001, ****P<0.0001.

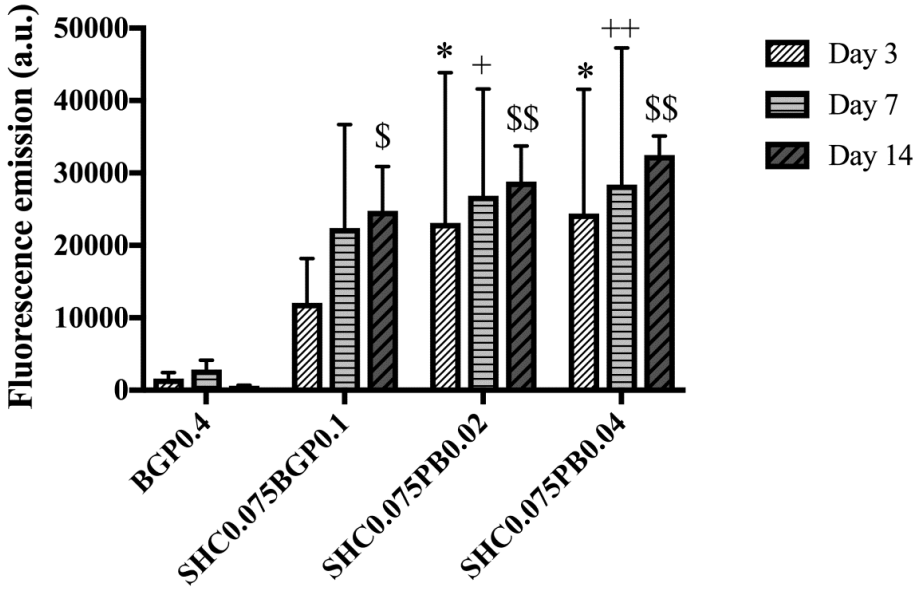

Figure S2. **Metabolic activity of the cells encapsulated in hydrogels after 3, 7 and 14 days.** Mean ± SEM (N=4, n=1). * p<0.05 compared to BGP0.4 at day3, + p<0.05 and ++ p<0.01 compared to BGP0.4 at day 7, $ p<0.05 and $$ p<0.01 compared to BGP0.4 at day 14.

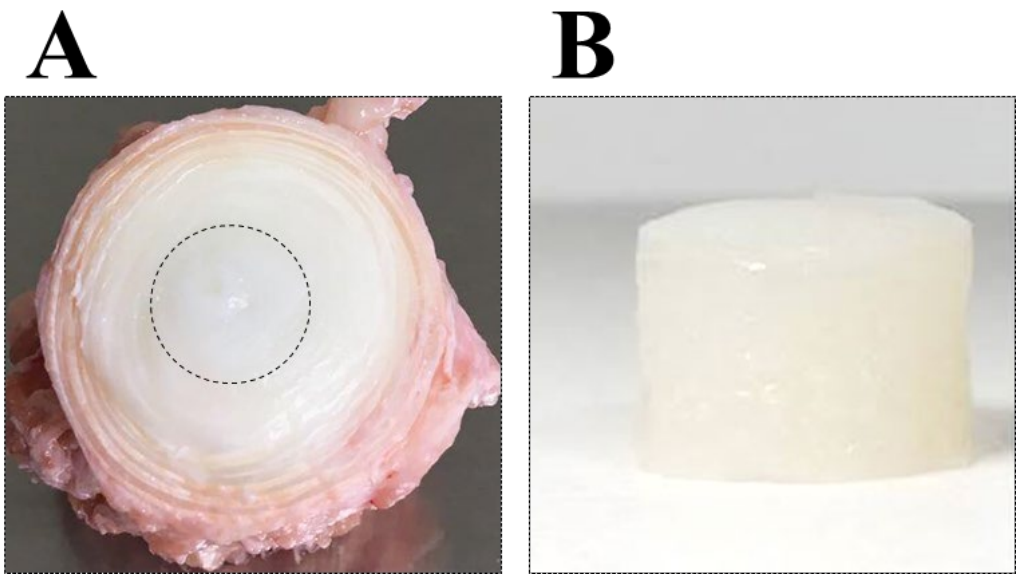

Figure S3. **Chitosan hydrogels have a similar appearance to the NP tissue**. Photograph of (A) a bovine intervertebral disc. The dashed-line circle shows the nucleus pulposus and (B) a chitosan hydrogel after 24h gelation at 37°C.